Available online at www.sciencedirect.com
ScienceDirect
International Journal of Thermal Sciences 47 (2008) 1688–1700
International Journal of Thermal Sciences
www.elsevier.com/locate/ijts

Fast heat release characterization of a diesel engine

Usman Asad, Ming Zheng *

Mechanical, Automotive and Materials Engineering, University of Windsor, 401 Sunset Ave, Windsor, Ontario N9B 3P4, Canada

Received 24 October 2007; received in revised form 18 January 2008; accepted 23 January 2008

Available online 4 March 2008

Abstract

Multi-event fuel injection strategies under independently controlled exhaust gas recirculation and intake boost have been applied to produce the heat release patterns that characterize the clean combustion techniques of modern diesel engines. Extensive experimental and analytical comparisons have been performed to better estimate the heat release characteristics from the cylinder pressure traces. A number of heat release models based on the First Principles are compared against a comprehensive heat release model, on the basis of numerical complexity and the ability to characterize the combustion process. Such study indicated that though the estimation from the simplified models is efficient when the heat release is close to the end of the cylinder compression stroke, the simplified models produce shortfalls in estimating the more spread multi-event heat release from the newer combustion systems. A new computationally efficient algorithm, based on the Diesel Pressure Departure Ratio, is proposed to characterize the various heat release patterns with adequate accuracy. The improved heat release analyzing algorithms are further programmed on real-time deterministic devices that process the cylinder pressure data to provide the necessary feedback for the fuel-injection model running on subsequent real-time controllers. The efficacy of the new algorithms has been experimentally demonstrated against selected cases of boost, engine load and exhaust gas recirculation on a modern diesel engine.

Keywords: Heat release; Diesel engine; Diesel pressure departure ratio; Combustion; Adaptive control

1. Introduction

The process of heat release can largely reflect the performance and emission characteristics of a diesel engine, when certain additional information is available such as the exhaust oxygen concentration, engine load level or ignition delay [1]. The mid heat release of conventional diesel engines has traditionally been phased close to the end of the compression stroke i.e. the top dead centre (TDC) and commonly with a profile of single hump or double humps for light and heavy load operations, respectively. A number of phenomenological models for the steady-state heat release analysis can be found in the literature [2–7]. Such models are normally capable of calculating the heat release characteristics of the conventional diesel combustion with sufficient accuracy [7–10]. However, the modern diesel engines utilize a multitude of advanced combustion strategies to enable compliance with the diesel emission norms. The current trend has been to split the heat release into multi-events or even to shift the heat release away from the TDC in order to lower the combustion temperature when low emissions of oxides of nitrogen (NOx) or low noise are targeted [11–15].

The phasing could be early (before TDC) or late (after TDC), for example, to accommodate high boost pressure and heavy exhaust gas recirculation (EGR) under high engine loads. Fig. 1 shows the experimental heat release rates for a number of fueling strategies and alternate combustion modes, recently obtained from the authors' laboratory during light-duty diesel research. It can be seen that the phasing and the duration of the heat release can vary extensively depending upon the mode of operation. For example, the noise control may be achieved with split injection events while a delayed phasing is necessary with high boost pressure to reduce the maximum cylinder pressure. Post flame control may also be employed for torque modulation or the destruction of soot in certain cases [16]. Since the previous heat release analysis techniques were developed for the conventional cases when the phasing is close to the best

* Corresponding author. Tel.: +1 519 253 3000x2636; fax: +1 519 973 7007.
E-mail address: mzheng@uwindsor.ca (M. Zheng).

1290-0729/$ – see front matter
doi:10.1016/j.ijthermalsci.2008.01.009

Nomenclature

CA50	Crank angle of 50% heat released
CA P_{max}	Crank angle of maximum pressure
CA$(dP/d\theta)_{max}$	Crank angle of maximum rate of pressure rise
$dP/d\theta$	Rate of pressure rise
$(dP/d\theta)_{max}$	Maximum rate of pressure rise
°CA	Crank angle in degrees
AHRR	Apparent heat release rate
ATDC	After top dead centre
BL	Baseline
CMPD	Compound combustion mode
Cum. HR	Cumulative heat released
DH	Double hump combustion mode
DIFF	Diffusion controlled combustion mode
EGR	Exhaust gas recirculation
EOC	End of combustion
FPC	Fired pressure characterization coefficient
h	Specific enthalpy ..... J/kg
HCCI	Homogenous charge compression ignition
IMEP	Indicated mean effective pressure
K	Combustion duration
LTC	Low temperature combustion
m	Mass ..... kg
MFB	Mass fraction burnt
MPC	Motored pressure characterization coefficient
n	Polytropic index
p	Pressure ..... Pa
PDR	Diesel Pressure Departure Ratio
Q	Energy transfer or release amount ..... J
RW	Rassweiler–Withrow model
SH	Single hump combustion mode
SOC	Start of combustion
T	Mean charge temperature ..... K
TDC	Top-dead-centre
u	Specific internal energy ..... J/kg
V	Volume ..... m^3

Greek symbols

γ	Ratio of specific heat/gamma
θ	Crank angle

Subscripts

app	Apparent
c	Charge
comb	Combustion
gr	Gross
ht	Heat transfer
mot	Motored
v	Volume

fuel efficiency timing, the impact of the combustion off-phasing and splitting on the heat release analysis needs to be evaluated.

The combustion examples presented in Fig. 1 include a significant premixed combustion part. This is typical of light-duty operation with high injection pressures so that the injection event is separated from the combustion and the longer ignition delay results in a large premixed part. With alternate fuels like bio-diesel, the higher cetane number reduces the ignition delay and the premixed phase is low compared to the diffusive part. The same is true for heavy-duty, high load operation where the combustion can be purely diffusive.

Additionally, the lowered combustion temperature prevalent during alternate combustion modes like HCCI and low temperature combustion (LTC) may reduce the combustion efficiency that is manifested by the increase in the emissions of carbon monoxide (CO) and unburnt hydrocarbons (HC) under extreme conditions. Lubricating oil dilution can also be another significant attribute of the combustion inefficiency. The empirical results for such an operating regime are given in Fig. 2, which shows the consecutive 200 pressure traces and the 200 cycle-averaged heat release rate for neat bio-diesel experiments [17]. The off-phasing of the heat release from the TDC and the use of multi-event combustion imply that the heat release may be significantly affected by the extended change in the cylinder volume (increased surface area for heat transfer), and the high CO and HC emissions. With the simplified heat release algorithms (constant specific heat ratio and neglecting the cylinder charge-to-wall heat transfer), the general shape of the heat release curve may still be attained but the magnitudes of the heat release rates are incorrect [7,8]. While normalizing the cumulative heat release (Cum. HR) with the total apparent energy release simplifies the analysis by not considering the effects of the combustion inefficiency, nevertheless, the uncertainty in the calculated combustion phasing and hence the estimation of the crank angle of 50% heat released (CA50) which is of paramount importance for control purposes may be increased.

Moreover, the implementation of such combustion modes is challenging due to the higher cycle-to-cycle variation of heavy EGR operation and the narrower operating corridors. While the transition from the high temperature combustion (HTC) to the LTC regime is relatively easier to control, maintaining stable engine operation in the LTC mode is generally not possible as shown in Fig. 3. Therefore, it is preferable to apply adaptive control to lock the phasing of the combustion process in a desired crank angle window to alleviate the problems associated with cyclic dispersion and to stabilize the combustion process. Previous research by the authors has shown that adaptive diesel combustion control strategies have the potential to navigate through the narrow operating corridors for achieving low emissions of NOx and soot while maintaining stable engine operation [14,18,19]. To enable adaptive control, the fast heat release calculation should be able to capture the transient nature of the combustion and provide the necessary feedback for control. However, the cycle-by-cycle calculation in real-time of the heat release characteristics in the above perspective is quite

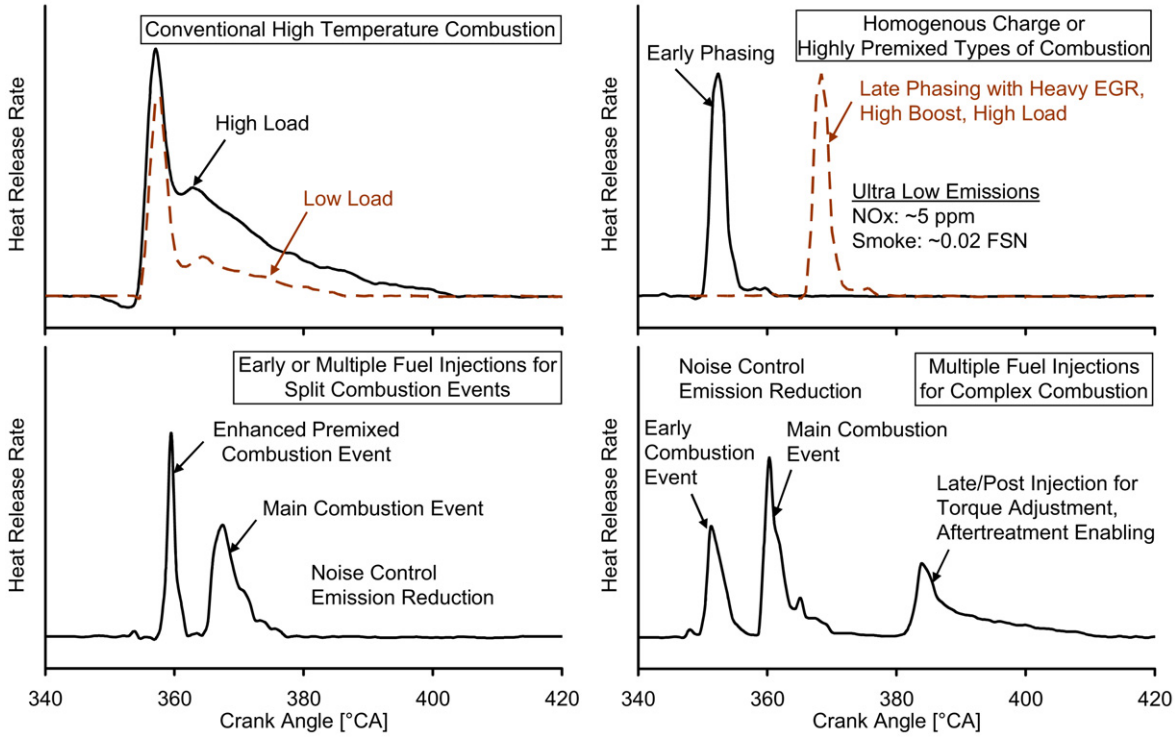

Fig. 1. Heat release rates for modern diesel engines.

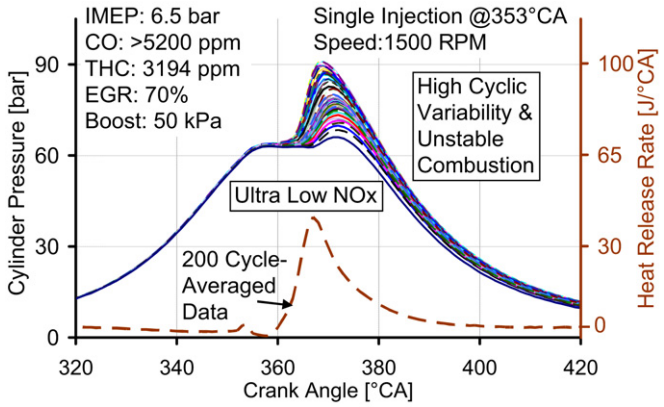

Fig. 2. Unstable combustion due to lowered flame temperature with heavy EGR.

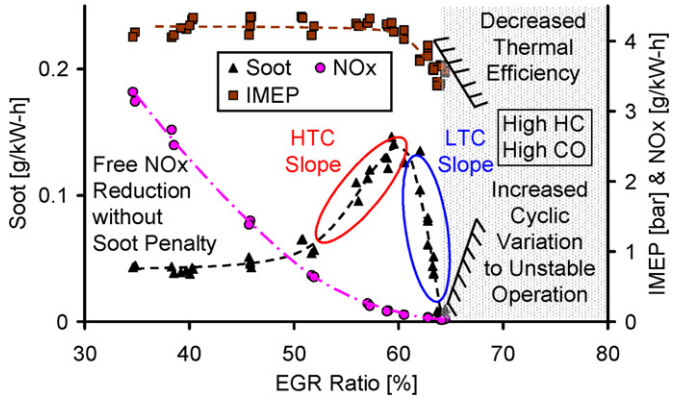

Fig. 3. Transition from high temperature combustion to low temperature combustion.

a challenging task. While the existing heat release models typically work well for general laboratory data analysis, their use in combustion control applications requiring on-the-fly calculation of the heat release is difficult because of the numerical complexity and computational time-constraints.

The control problem is compounded by the complexities of the modern diesel combustion systems, as outlined below:

- Prompt response within a time interval of 0.1–0.2 ms.
- Increased technological sophistication (common rail high pressure injection systems with multiple fuel injections per cycle, variable geometry turbines, advanced EGR handling techniques).
- A wide variety of combustion modes including LTC, HCCI, and enhanced premixed combustion.
- Combustion phasing adjustment to address a number of issues including limiting the peak cylinder pressure, reduction of combustion noise/emissions and after-treatment control.

Spark-ignition engines with sequential port injection or direction injection typically require adjustments in the combustion system to be carried out within a window of about 1 ms on a cycle-by-cycle basis [20]. Therefore, a slower response of the control system to any transients (changes in the fueling, combustion phasing) is generally adequate to modify the combustion regime. However, for modern diesel engines, it is possible for the complete combustion event to finish within 1 ms, for example, in the case of homogenous charge compression ignition (HCCI) where the total burn duration is around 5–10°CA.

Moreover, when comparing the events of combustion and fuel delivery/injection along the timeline, the potential for exercising in-cylinder control exists within the same cycle based on the compression history and injection events. Therefore, for realizing control within the same combustion cycle, the effective opening available for the in-cylinder control system to respond to any transients and make the necessary adjustments is usually around 0.1–0.2 ms.

The cycle-by-cycle adaptive control of the diesel combustion process requires a robust and fast feedback that can effectively identify the heat release characteristics. The heat release phasing is often used as the main feedback signal since it can be directly correlated to the combustion efficiency, emissions or power production capability [21,22]. Therefore, experimental and analytical comparisons have been performed to estimate the characteristics of heat release from the cylinder pressure histories. A number of heat release models such as apparent heat release model, Rassweiler–Withrow model, and Diesel Pressure Departure Ratio model have been investigated under the various cycle conditions. The emphasis of this research is on the fast and accurate estimation of the heat release phasing over a wide range of engine operating conditions on a cycle-by-cycle basis, and therefore, the key issues addressed in this paper are as follows:

- Analysis of a number of cylinder-pressure derived parameters for representing the heat release phasing.
- Implementation of a new computationally efficient algorithm for estimating the heat release characteristics and its performance comparison with other models.
- Demonstration of the efficacy of the new algorithm against selected cases of boost, engine load and exhaust gas recirculation on a modern diesel engine.

The cylinder-pressure derived parameters and heat release characteristics considered as the desired feedback include the crank angle of maximum pressure (CA P_{max}), the crank angle of maximum rate of pressure rise (CA$(dP/d\theta)_{max}$), and the crank angle of 50% heat released. The adaptive control tests using these feedback parameters have been run on a modern Ford common rail diesel engine coupled to an eddy current dynamometer. The details of the adaptive control strategy and the preliminary results for the adaptive control of diesel combustion using CA P_{max} and CA$(dP/d\theta)_{max}$ have been reported by the authors previously [18,19].

2. Analysis of heat release models

2.1. Heat release phasing feedback

The selection of the feedback parameters can strongly influence the dynamics of the closed-loop adaptive control system. The selection is constrained by the speed and capacity of an engine control unit and the numerical complexity of the control algorithms. Requirements for a practical feedback for the cycle-by-cycle control of combustion phasing are that it is accurate, stable and feasible for real-time control. Therefore, a comparison of the following parameters has been made on the basis of numerical complexity, applicability to different fueling strategies, shape of the heat release curve and the relative accuracy.

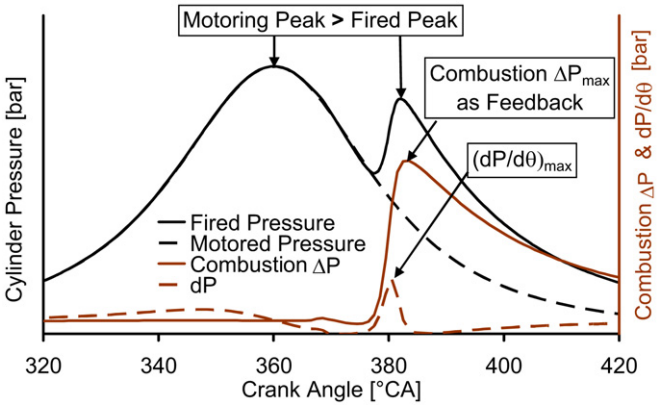

Fig. 4. CA P_{max} and $(dP/d\theta)_{max}$ as the feedback parameters.

- Crank angle of maximum cylinder pressure.
- Crank angle of the maximum rate of pressure rise.
- Crank angle of 50% heat released.

2.1.1. Crank angle of maximum cylinder pressure

This is the simplest of the parameters as it requires minimum computational resources. The use of CA P_{max} as a rough estimation of the heat release phasing is only valid when a global maximum pressure due to combustion occurs such as in case of HCCI/LTC combustion or with single-shot conventional high temperature combustion. With early or late combustion, or multiple injection events per cycle, CA P_{max} is a poor representation of the heat release phasing since it is closely coupled to the combustion volume. The accuracy of the CA P_{max} can be somewhat improved by subtracting the motored pressure from the fired pressure. The new pressure curve, thus obtained, represents the change in the cylinder pressure due to combustion and would provide a better estimate for late combustion phasing of conventional diesel combustion as shown in Fig. 4.

2.1.2. Crank angle of maximum rate of pressure rise

The performance of CA$(dP/d\theta)_{max}$ is similar to the CA P_{max} as far as providing an estimate for the heat release phasing is concerned. However, there are a few aspects that need to be mentioned. First, it is slightly more resource consuming than the calculation of CA P_{max}. Moreover, since it is the derivative of the pressure, it can provide a slight improvement in determining the location of the peak value compared to the maximum pressure. For late combustion timing, the accuracy can be improved by subtracting the motoring $dP/d\theta$ trace from the fired $dP/d\theta$, to obtain the combustion $dP/d\theta$ only. However, if the combustion is rough or the pressure transducer is not flush-mounted in the cylinder head, the noise in the pressure signal is amplified during the calculation of the $(dP/d\theta)_{max}$, resulting in large errors in the estimation of the heat release phasing. Therefore, filtering or smoothing of the pressure signals becomes necessary.

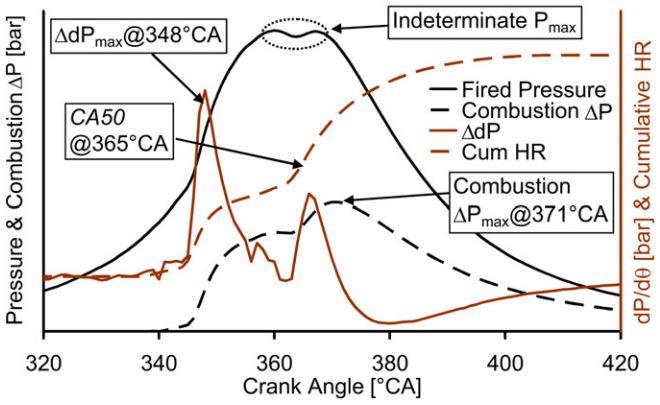

Fig. 5. Comparison of the feedback parameters for a split heat release pattern.

2.1.3. Crank angle of 50% heat released

Although diesel engines are overall lean-burn systems, the combustion is predominantly and locally stoichiometric burn, because the flames tend to initialize and propagate to approximately stoichiometric regions. Therefore, the heat release slope is generally steep and the CA50 represents a stable and robust measure of the phasing of combustion, compared to CA $P_{\max}$ and CA$(\mathrm{d}P/\mathrm{d}\theta)_{\max}$, as shown in Fig. 5. However, the calculation of the CA50 is computationally quite intensive and therefore, simplifications to the heat release analysis are generally made to reduce the numerical complexity while maintaining sufficient accuracy of the calculation. Therefore, three heat release models for estimating the CA50 with varying degrees of complexity and accuracy have been considered in the following section.

2.2. Heat release modeling

The basis for the modeling of the heat release is the first law of thermodynamics for an open system. Assuming the cylinder charge as a single zone and using the ideal gas law, the heat release during combustion, $\mathrm{d}Q_{\mathrm{gr}}$ on a crank angle basis is given by:

$$\frac{\mathrm{d}Q_{\mathrm{gr}}}{\mathrm{d}\theta} = \frac{1}{\gamma-1}\left[\gamma p\frac{\mathrm{d}V}{\mathrm{d}\theta} + V\frac{\mathrm{d}p}{\mathrm{d}\theta} + (u - c_v T)\frac{\mathrm{d}m_c}{\mathrm{d}\theta}\right] - \sum h_i\frac{\mathrm{d}m_i}{\mathrm{d}\theta} + \frac{\mathrm{d}Q_{\mathrm{ht}}}{\mathrm{d}\theta} \quad (1)$$

where m_c is the mass of the cylinder charge, c_v is the specific heat at constant volume, u is the specific internal energy, T is the mean charge temperature, p is the cylinder pressure, V is the cylinder volume, γ (gamma) is the ratio of the specific heats, $\mathrm{d}Q_{\mathrm{ht}}$ is the charge-to-wall heat transfer and $\sum h_i m_i$ represents the enthalpy flux across the system boundary.

Eq. (1) gives the gross heat release rate during the period from intake valve closure (IVC) to exhaust valve opening (EVO) for the crank angle interval, $\mathrm{d}\theta$. It also forms the basis for three different heat release models of reduced levels of complexity that have been analyzed in this paper. The detailed information on the First Law equation derivation and the implicit assumptions can be found in the literature [4–8].

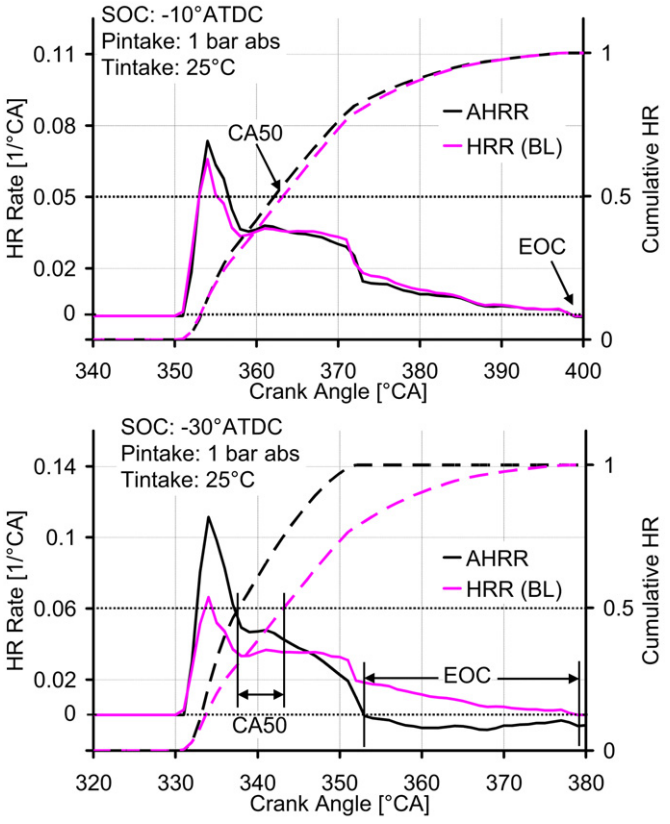

Fig. 6. Apparent heat release analysis; Upper: SOC@−10°ATDC; Lower: SOC@−30°ATDC.

2.2.1. Apparent heat release model

By neglecting the heat transfer, crevice volume, blow-by and the fuel injection effects in Eq. (1), the resulting heat release rate is termed as the apparent or net heat release rate, $\mathrm{d}Q_{\mathrm{app}}$ [4–8]. Substituting $\mathrm{d}Q_{\mathrm{app}} = \mathrm{d}Q_{\mathrm{gr}} - \mathrm{d}Q_{\mathrm{ht}}$ and $\mathrm{d}m_c = \mathrm{d}m_i = 0$, Eq. (1) gives the apparent heat release rate (AHRR) as follows:

$$\frac{\mathrm{d}Q_{\mathrm{app}}}{\mathrm{d}\theta} = \frac{\mathrm{d}Q_{\mathrm{gr}}}{\mathrm{d}\theta} - \frac{\mathrm{d}Q_{\mathrm{ht}}}{\mathrm{d}\theta} = \frac{1}{\gamma-1}\left[\gamma p\frac{\mathrm{d}V}{\mathrm{d}\theta} + V\frac{\mathrm{d}p}{\mathrm{d}\theta}\right] \quad (2)$$

The cumulative apparent heat release (Cum. AHR) is obtained by summing the incremental values from Eq. (2) over the combustion period. Apparent heat release values are typically 15% lower than those obtained on a gross heat release basis [6,8]. Apparent heat release values are very often used in preference to gross heat release values because this reduces the amount of computation and avoids the need for heat transfer parameters to be specified. Although the apparent heat release analysis generally provides reasonable accuracy for heat release phased close to the TDC, however, under certain operating conditions, it can lead to errors in the calculated results as shown in Fig. 6.

The baseline (BL) heat release rate is calculated using Ricardo Wave software and Synthetic Atmosphere Engine Simulation (SAES) software developed by one of the authors [23]. The SAES uses a comprehensive validated model for heat release calculations and includes the effect of heat transfer, crevice volume, charge composition etc. on the heat release rate. For the case with start of combustion (SOC)@−30°ATDC,

a considerable difference in the magnitudes of the heat release rates and a large deviation in the end of combustion (EOC) are observed between the baseline curve and the AHRR curve. Since the calculation of the CA50 with the apparent heat release approach requires an accurate estimation of the EOC crank angle, a large error is observed in the calculation of the CA50.

2.2.2. Rassweiler–Withrow model

The Rassweiler–Withrow model (referred to as RW model) is commonly used to estimate the mass fraction burnt (MFB) and can be taken as a normalized version of the cumulative heat released [24–26]. It is based on the assumption that the change in pressure due to the piston motion and charge-to-wall heat transfer can be represented by polytropic processes. In this method, the pressure change during any crank angle interval is assumed to be made up of a pressure rise due to combustion Δp_{comb} and a pressure rise due to the volume change Δp_v. Therefore, by assuming that the pressure rise due to combustion is proportional to the mass of the fuel that burns, the MFB at the end of the jth interval can be approximated by

$$\text{MFB}_{\text{RW}}(j) = \sum_{i=0}^{j} \Delta p_{\text{comb}}(i) \Big/ \sum_{i=0}^{K} \Delta p_{\text{comb}}(i) \tag{3}$$

where K is the total combustion duration. The incremental heat release rate can also be calculated as follows:

$$\Delta Q(j) = (V_j/n - 1)\Delta p_{\text{comb}}(j) \tag{4}$$

where

$$\Delta p_{\text{comb}}(j) = p_j - p_{j-1}(V_{j-1}/V_j)^n \tag{5}$$

The cumulative heat released can then be calculated as for the apparent heat release model. The detailed information on the RW model derivation is given in Refs. [6,24,25]. A constant value (1.37) of the polytropic index, n, has been used for the analysis. The computation of the RW MFB is somewhat simpler than the cumulative apparent heat release calculation. Therefore, the use of the RW model has been limited to the calculation of the MFB as an approximation of the normalized cumulative heat released and the resulting CA50.

2.2.3. Diesel Pressure Departure Ratio model

The Diesel Pressure Departure Ratio algorithm (referred to as PDR algorithm hereafter) is a new approach proposed by the authors for fast and reliable estimation of the mass fraction burnt for diesel combustion. It is based on the principle of RW model which states that the fractional pressure rise due to combustion can provide an estimate of the MFB. The PDR algorithm utilizes the fired and the motoring races for cycle-by-cycle estimation of the CA50 and the MFB closely matches the normalized cumulative heat release trace.

The authors would like to mention that a somewhat similar approach has been applied for spark-ignition engines by Sellnau [27] and Matekunas [28], and is called the Pressure-Ratio Management (PRM). PRM involves the calculation of the ratio between the fired pressure and the corresponding motored cylinder pressure at every crank angle. The ratio is then normalized by its maximum value (also called the final pressure ratio) which typically occurs around 55°CA ATDC for spark-ignition engines. The resulting trace is a close approximation of the MFB trace at every crank angle and published results indicate that the technique works well for spark ignition engines.

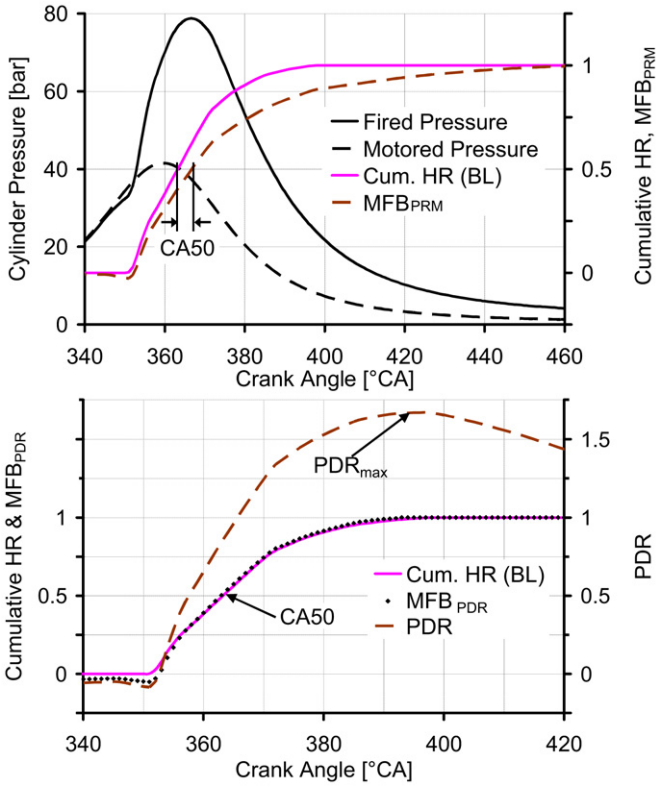

Fig. 7. Upper: MFB_{PRM}, lower: MFB_{PDR} for the same data.

The direct application of the PRM to diesel engine pressure data results in a MFB curve that may differ from the actual cumulative heat release trace because of a number of reasons. First, the much higher compression ratios of the diesel cause the maximum pressure ratio to occur towards exhaust valve opening. Second, unlike the spark ignition engines where the combustion typically occurs as a single event, the diesel combustion process can consist of discrete heat release events due to a variety of fuel injection scheduling strategies (split injections, post injection, etc.). Therefore, the PRM estimation departs from the actual diesel combustion characteristics even for the conventional high temperature diesel combustion with a single fuel injection as shown in the upper part of Fig. 7.

To identify the diesel combustion characteristics, the authors have introduced a Diesel Pressure Departure Ratio (PDR) that is expressed at any crank angle, θ as:

$$\text{PDR}(\theta) = f\{P(\theta), P_{\text{mot}}(\theta), V(\theta), n, C_1, C_2\} \tag{6}$$

where $P(\theta)$ is the fired cylinder pressure data, $P_{\text{mot}}(\theta)$ is the motored cylinder pressure data, $V(\theta)$ is the cylinder volume, n is the polytropic index and C_1, C_2 are constants.

For the current analysis, a numerically reduced form of Eq. (6) that is computationally efficient has been used and is given as:

$$\text{PDR}(\theta) = \frac{P(\theta) + \text{FPC}}{P_{\text{mot}}(\theta) + \text{MPC}} - 1 \tag{7}$$

where FPC is the 'fired pressure characterization' coefficient, and MPC is the 'motored pressure characterization' coefficient. The coefficients, FPC and MPC are constants for a given engine configuration and are largely not affected by the boost pressure, EGR, etc. as is shown later in the PDR algorithm performance tests. The PDR has a nearly zero value before combustion and rises to maximum value which corresponds to the end of combustion (EOC).

An estimate of the mass fraction burnt is then obtained by normalizing the PDR from Eq. (7) with its maximum value PDR_{max} as follows:

$$MFB_{PDR}(\theta) = \frac{PDR(\theta)}{PDR_{max}} \tag{8}$$

To illustrate the PDR algorithm, the calculated PDR and the MFB_{PDR} are shown in lower part of Fig. 7 for the same data as in the upper part. It can be seen that the PDR reaches a maximum value close to the crank angle where the combustion ends. Also the MFB_{PDR} is in good agreement with the baseline normalized cumulative heat release trace which includes the effects of charge-to-wall heat transfer and the temperature dependence of the specific heat ratio.

The empirical model constants (FPC and MPC) are calibrated by first adjusting the MPC value so that the MFB_{PDR} approximately matches the baseline heat release trace. Small changes in the MPC value cause the curve to pivot about a point. The FPC is then adjusted to shift the pivotal point as close as possible to the CA50. This ensures that small deviations on the extreme ends of the curve will have minimal effect on the prediction of the CA50. The calibrated values of the constants are then checked against few traces representing early/late phasing and different fueling strategies. Once this trial and error process is completed, the constants have been calibrated for the engine under consideration and are not required to be adjusted. Using the procedure outlined above, the calibrated values of MPC and FPC were 4.8 and 4.0, respectively, for the test engine used in the experimental investigation.

3. Experimental apparatus and procedures

A number of researchers have previously carried out an analysis of the apparent heat release model for errors in the gross heat released (in joules) due to constant gamma, heat transfer and pressure data errors [6,7,29–32]. However, the pressure data used was typical of the conventional high temperature combustion regime for both low-load and high-load diesel operation. The modern diesel engines utilize multiple injections per cycle and unconventional combustion modes like HCCI, LTC. Moreover, for control applications, the phasing of the heat release (given by CA50) is of far more importance than the absolute value of the heat released. Therefore, the prediction of the apparent heat release model needs to be critically analyzed in this new perspective. Moreover, for feedback-control purposes, a compromise must be made between the required accuracy and the system resource constraints such that the simplest algorithm with the minimum required accuracy can be implemented for real-time control.

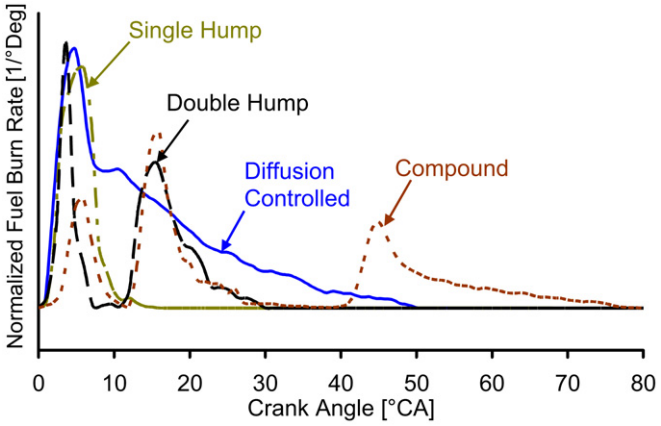

Fig. 8. Fuel burn rate patterns.

The methodology for evaluation of the errors with the assumption of a constant gamma value and neglecting the heat transfer has been investigated for four different fuel burn rate patterns as shown in Fig. 8. These burn rates are adapted from empirical data and comprehensively summarize the modern diesel combustion operating regimes.

These fuel burn rate patterns are categorized as follows:

- Diffusion controlled mode (DIFF) – corresponding to conventional high temperature diesel combustion.
- Single hump (SH) – representing homogenous charge or highly premixed types of combustion modes.
- Double hump (DH) – representing split combustion events by fuel injection strategies including early or multiple injections.
- Compound (CMPD) – representing complex combustion by split injections along with late/post injections for enabling aftertreatment or soot destruction.

The evaluation of the errors in this paper has been carried out using both simulated and experimental pressure data. The fuel burn profiles of Fig. 8 were entered as the user-defined fuel burn rate input to generate the simulated pressures using Ricardo Wave and SAES softwares. The calculated gross heat release from the softwares and the resulting CA50 was taken as the baseline reference against which all errors have been evaluated. A timing sweep was performed for each of the four burn rates by varying the start of combustion (SOC) from −30°CA ATDC to 30°CA ATDC. The motored pressure used during the analysis was calculated by starting with a baseline experimental motoring pressure trace for naturally aspirated conditions at zero EGR and correcting it for boost and EGR using the fired pressure trace. The effect of charge-to-wall heat transfer, trapped residual mass, etc. is therefore accounted for. The details of this technique are explained in the RT-FPGA programming section of the paper. The test engine specifications are given in Table 1 and the same have also been used in the simulations. The assumed engine operating conditions are given in Table 2.

Table 1
Geometric characteristics of the test engine

Type	4 cylinder, 4 stroke cycle diesel engine
Bore × stroke	0.086 m × 0.086 m
Displacement	1.998 litres
Compression ratio	18.2:1
Combustion system	Direct injection
Injection system	Common rail (up to $P_{Rail} \sim 160$ MPa)

Table 2
Engine operating conditions

Engine speed	1200 rpm
Intake pressure	1 bar abs
Intake temperature	298 K
Injection timing	−35°CA ATDC → 25°CA ATDC (10° Increment)
Ignition delay	5°CA
Burn duration	10° → 80°CA
Residual fraction	0.08
Combustion efficiency	100%

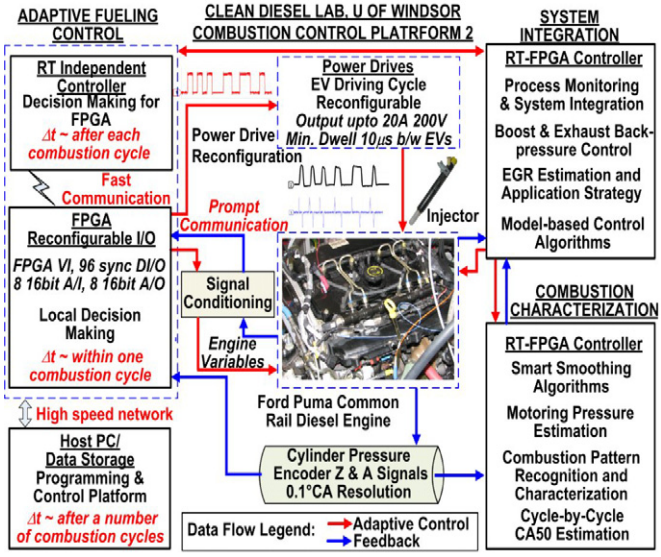

Fig. 9. RT-FPGA systems for real-time control of diesel engines.

3.1. PDR algorithm application

The experiments have been performed on a single cylinder of a four-cylinder Ford Puma common-rail diesel engine (see Table 1 for specifications). The details of the separation of the single cylinder from the rest of the cylinder have been reported previously [33]. A dual-bank exhaust analyzer system (NOx, HC, CO, CO_2, O_2, and soot) has been instrumented for the tests; normally one for the exhaust emissions and the other for the intake gas concentrations. The intake air is supplied from an oil-free dry air compressor. The engine boost, exhaust back-pressure, and EGR valve opening are automated with on-line digital control. The engine coolant and lubricating oil conditions are retained closely with external conditioning systems to minimize the discrepancies of the testing results.

The PDR algorithm has been programmed on a National Instruments' Real-time (RT) embedded controller with a field programmable gate array (FPGA) device that conditions the cylinder pressure signal, processes/analyzes the data and provides the necessary feedback to the fuel-injection model running on subsequent RT-FPGA controllers. An overview of the RT-FPGA systems for control of diesel engines is given in Fig. 9.

The RT-FPGA hardware provides a deterministic platform for fast data acquisition with a large computational capacity and reliable control at loop speeds up to 40 MHz. Therefore, for an engine running at 3000 RPM, the time available between a crank angle interval of 1°CA is ∼55 μs. The RT-FPGA platform can perform thousands of complex numerical operations during such short time intervals, thereby providing immense capacity and flexibility for deterministic execution of control algorithms. The authors have tested these systems up to their maximum capacity during adaptive fuel-injection control experiments, with multiple-injections per combustion cycle and the systems have performed without a malfunction.

A reliable feedback that is robust and minimally affected by external disturbances is essential for acceptable performance of the model-based algorithms. The computation of the feedback should be fast enough to capture the characteristics of each combustion cycle and the algorithm for the feedback estimation should be able to capture the effect of changes in the engine operating conditions. Therefore, the experimental results presented investigate the robustness of the PDR algorithm against variation in a number of engine variables.

The uncertainties in the pressure and the crank angle measurement can affect the performance of the heat release algorithms. The major cause of the uncertainty is electrical noise which may result in significant errors in the measurements. Another cause is the signal drift of piezo-electric pressure transducers. The authors use hardware filtering and shielded cables to reduce the electrical noise and pressure pegging techniques to minimize the errors due to the sensor drift. The crank angle measurement is referenced against the encoder Z Index every engine revolution which normally limits the maximum measurement uncertainty to 0.1°CA.

3.2. RT-FPGA programming

The FPGA code [14,18,19] acquires the cylinder pressure (16 bit resolution) with a crank angle resolution of 0.1°CA and performs a number of operations including detection and elimination of external noise in the data (if required) and estimation of the motoring cylinder pressure trace. The calculation of the MFB_{PDR} and CA50 is then carried out on a cycle-to-cycle basis and the value is passed on to the adaptive fuel injection control algorithms on subsequent FPGA controllers, to enable control of the next combustion cycle.

The baseline condition, for instance, the motoring pressure for naturally aspirated or turbocharged conditions at zero or high EGR is programmed into the FPGA memory (4 kB block size with 16 bit resolution) at the start of the tests. The code execution occurs every time the external clock signal (Index A) from the engine-mounted encoder is detected. The key sequence of the calculation includes the following:

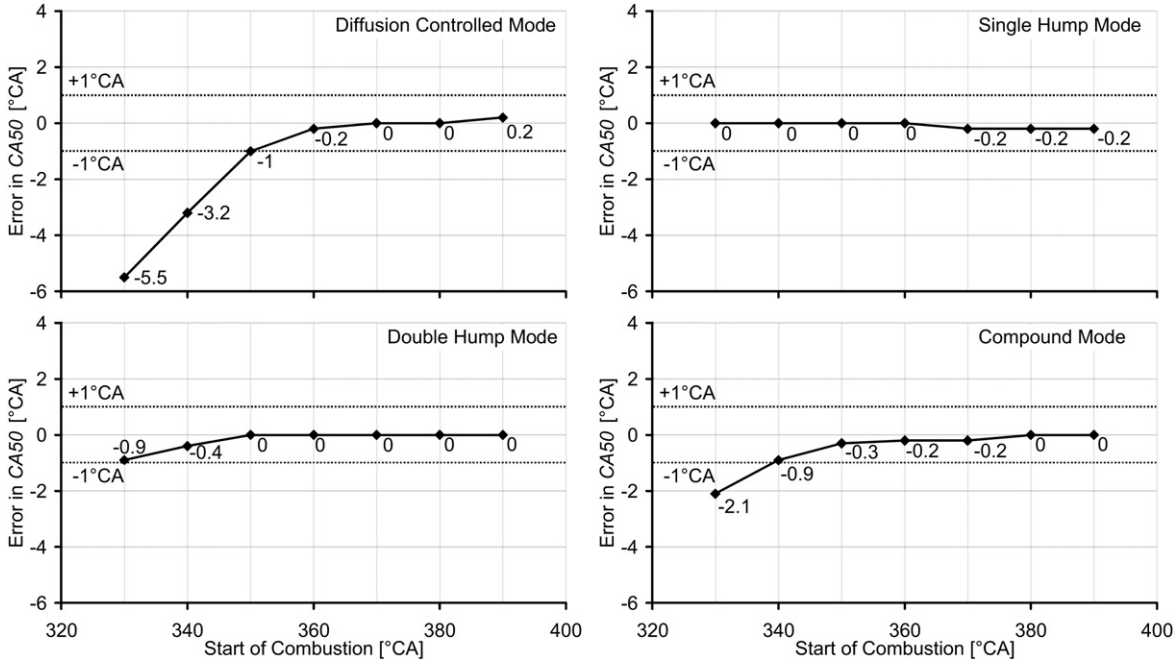

Fig. 10. Summary of the AHR error analysis.

- The pressure is pegged at −60°CA ATDC (no combustion) to automatically adjust the motoring trace for the current operating conditions (boost, intake temperature, EGR, etc.).
- A correction to the estimated motoring trace is made by referencing the actual pressure at −30°CA ATDC (no combustion). This enables the effect of EGR to be approximated in the motoring trace.
- The PDR trace is calculated for the crank angle window from −30°CA ATDC to 100°CA ATDC.
- The maximum value of the PDR is used to get the MFB_{PDR} trace.
- The crank angle corresponding to the CA50 is then identified and provided as feedback for control purposes.
- The calculation is then repeated for the next cycle.

4. Results and discussion

4.1. Evaluation of errors

Selected results for each of the four fuel burn rate patterns for the injection timing sweep from −35°CA ATDC to 25°CA ATDC (SOC from −30°CA ATDC to 30°CA ATDC) are given below. The apparent heat release rate (AHRR) computed with a constant gamma value of 1.37, is compared against the baseline (BL) results, as shown in Fig. 10. The error in the CA50 is considered to be negative if the model prediction is earlier than the baseline value. An error of ±1°CA or less has been considered as acceptable in this study and is indicated on the figure.

Diffusion controlled mode. The error in the prediction of the CA50 is large for the cases with the CA50 before the TDC. However, for combustion phasing at and after TDC, the prediction of the AHR model matches the baseline results. This can be attributed to the higher heat transfer rates for the early combustion because of the larger combustion chamber surface area and the sustained high temperatures due to the longer combustion duration (50°CA) and the ongoing compression process.

Single hump mode. A short combustion duration of about 10°CA and low-load operation is typical of homogeneous charge or highly premixed types of combustion modes. Since the combustion is quite rapid, the AHR analysis is able to effectively capture the combustion phasing. Therefore, the cumulative AHR traces match with the baseline results for all the timing sweep cases.

Double hump mode. The results shown are for a typical split injection strategy, with a ratio of the pilot injection to the main injection quantity equal to 0.7, and a dwell of 15°CA between the two injections. The cumulative AHR error in the early phased cases does not affect the calculated CA50 significantly as the less quantity of the pilot injection confines the error below the CA50 level. However, if a ratio greater than 0.8 is employed, significant errors may result in the CA50 calculations for the early phased cases.

Compound mode. The use of a post or late injection for enabling aftertreatment or destruction of soot has been categorized under the compound fuel-burn pattern. The simulated combustion duration is quite long, about 80°CA in this case. However, as long as the pilot and main injections represent the majority of the fuel injected, the error in the calculated values is small.

The largest error in the heat release calculation is most likely incurred by ignoring the charge-to-wall heat transfer. However, it can be seen that the AHR analysis provides a reasonable esti-

mate of the CA50 for all the four fuel burn patterns considered, for most of the timing sweep.

The error analysis was repeated with the RW model for the SOC timing sweep from −30°CA ATDC to 30°CA ATDC. The results for the four fuel burn patterns with the SOC at −10°CA ATDC are shown in Fig. 11. The MFB traces have been staggered on the x-axis (crank angle) for the same SOC to make the comparison easier to understand. The MFB traces show very good agreement for the first three fuel burn patterns. However, for the compound mode of combustion, the MFB_{RW} shows a deviation from the cumulative HR trace. Analysis of similar traces for different SOC revealed that for early combustion phasing, the error is similar to that observed with the AHR model. However, for the compound mode of combustion, a significant error is observed for all cases of the combustion phasing sweep.

For the compound mode, the combustion duration is 80°CA so that the combustion progresses well into the expansion stroke. At this stage, the change in pressure due to the volume change becomes significantly higher than that due to combustion, especially so because of the higher compression ratio of the diesel engine. Therefore, the assumption of a fixed polytropic index causes the MFB_{RW} to deviate significantly. Care should be taken in using the MFB_{RW} for delayed combustion phasing or for combustion modes with late injection events.

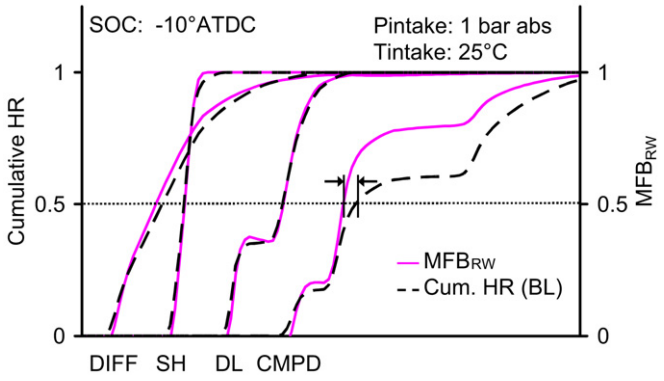

Fig. 11. Comparison of CA50 prediction between MFB_{RW} and Cum. HR.

The estimation of the CA50 using the MFB_{PDR} is presented for all the four modes of combustion in Fig. 12. The FPC and MPC are determined initially and kept constant through out the analysis. For the DIFF mode, the MFB_{PDR} shows large errors in the CA50 for the early SOC cases. For combustion starting around TDC, the results are similar to those obtained with the AHR analysis, and the MFB_{PDR} generally follows the baseline results except for the late SOC cases where a small deviation is observed. When the combustion duration is short (SH mode), the performance of both the AHR and the PDR models matches the baseline cumulative HR traces. As already discussed for the AHR model, the combustion phasing has negligible effect on the calculations of the simplified algorithms.

For the DH Mode, although deviations from the baseline results are observed similar to the AHR predicted traces, the estimation of the CA50 is not affected. The reasons for this have already been highlighted during the error analysis of the AHR model. For the compound mode, the MFB_{PDR} traces for the early phasing are similar to those from the AHR model. Unlike the results from the RW model, the MFB_{PDR} is able to capture the heat release characteristics for combustion phased around the TDC. However, for late combustion phasing with the CA50 occurring after 380°CA, the MFB_{PDR} traces deviate from the baseline results. Although such late phasing might be considered impractical for engine applications, nevertheless, the results indicate a limitation of the PDR model for compound type of heat release patterns with late phasing.

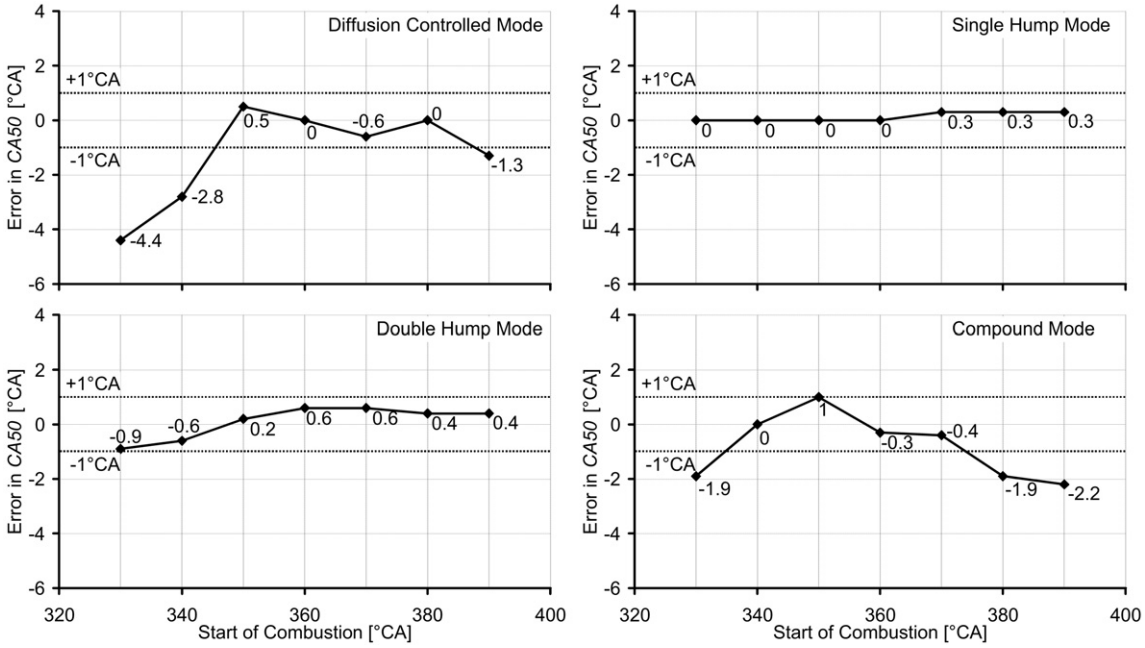

Fig. 12. Summary of the MFB_{PDR} error analysis.

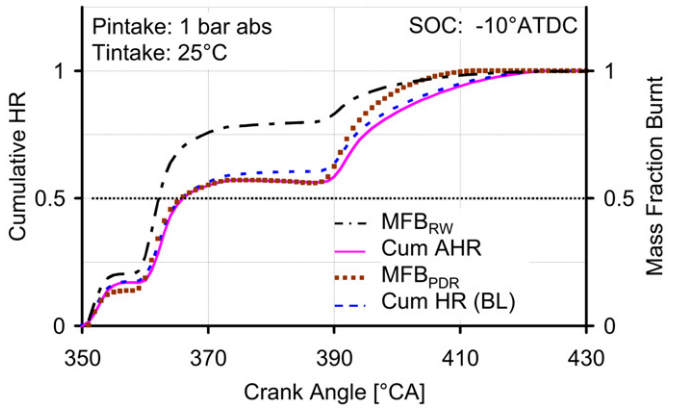

Fig. 13. Comparison between MFB_{PDR}, MFB_{RW} and AHR models (CMPD mode).

The PDR analysis provides a reasonable estimate of the CA50 for all the four fuel burn patterns considered, for most of the timing sweep. It can be seen that the results are quite similar to those obtained with the AHR model.

A comparison of the three models for the compound mode with SOC at −10°CA ATDC is shown in Fig. 13. Although being the simplest of the three models, the MFB_{PDR} is able to capture the CA50 with reasonable accuracy while the error with the RW model is significant. It is pertinent to add here that a situation may arise where the MFB value between the two combustion events (from 370 to 390°CA) may be 0.5. Although the PDR algorithm would predict 370°CA as the CA50 (the first crank angle at which the MFB value becomes 0.5), the CA50 determination in such cases would be imprecise. This also highlights the limitations of the CA50 as a measure of the combustion phasing under such combustion modes. The authors are working on alternate parameters/methodology for estimating the combustion phasing for such combustion regimes and the results will be reported in the near future.

4.2. *Quality of pressure data*

The quality of the pressure data can affect the prediction and thereby the robustness of the heat release models. The AHR model is more susceptible to pressure noise as it includes the derivative of the pressure which amplifies any noise present in the signal. This is clearly shown in Fig. 14 and has significant implications on the calculation of the cumulative heat released since it requires the EOC to be identified with reasonable accuracy. Therefore, heavy smoothing of the pressure data needs to be performed before any reasonable estimate of the CA50 can be made, which significantly increases the computational overheads. On the other hand, the PDR model is able to predict the CA50 with sufficient accuracy without any treatment applied to the pressure data. This makes the model more robust and suitable for real-time applications than the apparent HR model.

4.3. *PDR algorithm performance tests*

Additional experiments have been performed to demonstrate the PDR algorithm performance for selected cases with variation in boost, EGR, engine load, and fuel injection strategies. The baseline cumulative heat release has been calculated using both the AHR model and the comprehensive model including the heat transfer estimation and specific heat ratio variation with temperature. If a difference exists between these two models, then the baseline value shown in the figures represents the value from comprehensive HR model. High values of EGR are presented in these results to test the performance of the algorithm at the extreme conditions of EGR with high cycle-to-cycle variation and increased emissions of CO & HC so that the limitations of the model may be better identified.

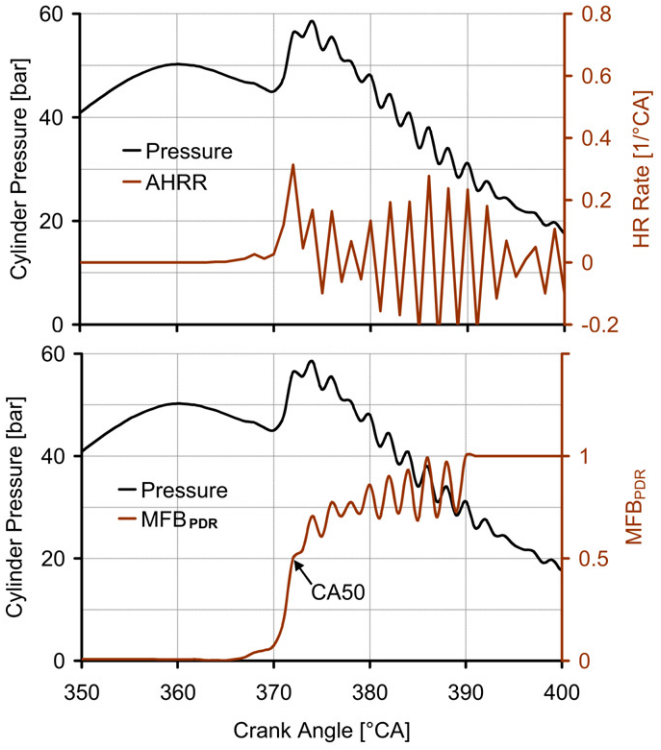

Fig. 14. Model comparison for a noisy pressure trace; Upper: AHRR; Lower: MFB_{PDR}.

The estimation of the motoring pressure trace can have a significant effect on the PDR model performance. The predicted motoring traces for different levels of EGR are shown in Fig. 15. High levels of EGR cause a reduction in the cylinder pressure during the compression stroke. The RT-FPGA code is able to track this trend and modify the motoring traces as the amount of EGR is changed. This also implies that the algorithm can to some extent, account for changes in the composition, the specific heat ratio and the charge-to-wall heat transfer.

The effects of EGR variation with a single injection per cycle on the MFB_{PDR} are shown in Fig. 16. As the amount of EGR is increased from zero to 56%, the combustion is progressively delayed. It can be seen that the model is able to accurately predict the retarded combustion phasing.

The effects of changing the boost pressure and the fuel injection strategy are shown in Fig. 17. With multiple injections per cycle (3 early injections and one main injection), the heat release curve takes the shape of the double hump pattern. The

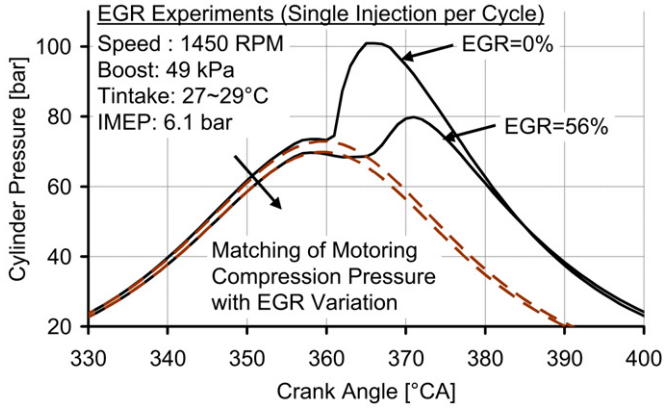

Fig. 15. Estimation of motoring pressure.

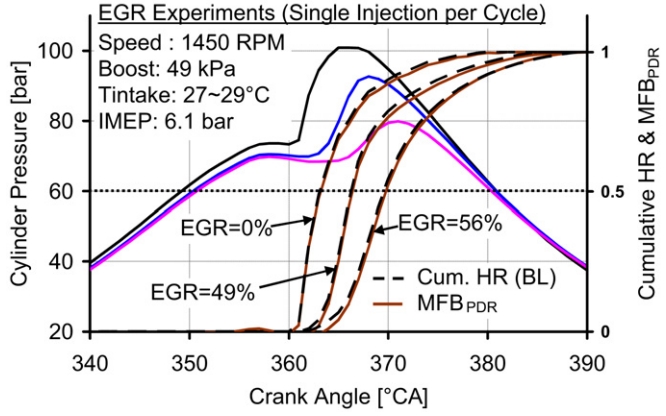

Fig. 16. EGR sweep experiments.

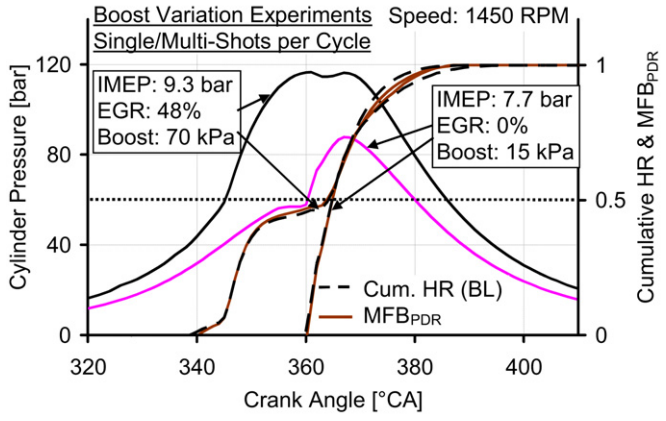

Fig. 17. Variation of boost & fuel injection strategy.

PDR model is able to reasonable predict the CA50 within the prescribed limits of accuracy, that is, ±1°CA.

The variation of the engine load with the boost pressure held constant is shown in Fig. 18. The low indicated mean effective pressure (IMEP) case represents the single hump type of combustion, while the higher load case falls in the double hump category. The PDR algorithm in these cases is also able to fairly predict the occurrence of the CA50.

The application of the PDR algorithm for various combustion modes and fuel injection strategies shows that the estimation of the heat release characteristics using the PDR algorithm is least affected by the combustion off-phasing and split combustion events. Moreover, the numerically simplified form of the PDR algorithm given in Eq. (7) provides normalized heat release comparable to the baseline and apparent heat release data at a reduced computational cost. An improved version of the PDR algorithm that will account for the energy loss with the high CO and HC emissions during low-temperature combustion and provide actual information about the cycle work is also under development by the authors.

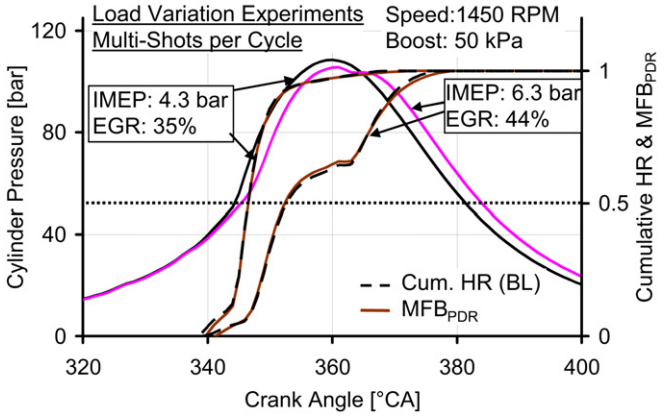

Fig. 18. Load variation experiments.

It is pertinent to mention here that while a modern personal computer could also be used for the cycle-by-cycle analysis, the RT-FPGA system ensures real-time determinism in the calculation which cannot be achieved with a Windows/Linux-based platform. The authors are in the process of computing the actual reduction in the computational time provided by the PDR algorithm, compared to the existing models using both Windows-based personal computers and RT-FPGA systems. The results of this study will be presented in the near future.

5. Conclusions

Theoretical and empirical investigations are carried out for the implementation of real-time heat release analysis that will provide feedback for cycle-by-cycle adaptive control of modern diesel combustion systems. The suitability of a number of cylinder-pressure derived parameters and heat release characteristics is discussed for real-time applications. The crank angle of 50% heat released was shown to represent a stable and robust measure of the phasing of the heat release patterns that characterize the clean combustion techniques of modern diesel engines. The heat release models based on the First Principles are analyzed as feedback on the basis of numerical complexity, applicability to different fueling strategies, and the relative accuracy in comparison with the comprehensive heat release model. An attempt has been made to identify those regions where the use of the simplified algorithms provides sufficient accuracy for control applications.

The new Diesel Pressure Departure Ratio Algorithm is a computationally efficient algorithm, proposed for estimating the crank angle of 50% heat released of each combustion cy-

cle. The PDR Algorithm is demonstrated to effectively estimate the phasing of the split/multi-event heat release pattern. Moreover, the prediction of the phasing by the PDR is almost as good as that obtained from the comprehensive heat release algorithms.

For computation in real-time, the PDR algorithm is suitable for implementation at the hardware level and was programmed with a set of RT-FPGA controllers. The hardware setup presented in this research has proved sufficient for the targeted real-time cylinder pressure analysis and provides an efficient platform for the future development work. The efficacy of the Diesel Pressure Departure Ratio algorithm was emulated and experimentally validated against selected cases of boost, engine load and exhaust gas recirculation on a modern diesel engine. It is pertinent to mention here that the comprehensive heat release analyzing algorithms cannot be implemented for real-time calculations, with the available resources of the RT-FPGA systems.

Acknowledgements

The authors are grateful for support from the University of Windsor, the Canada Research Chair Programme, the Natural Sciences and Engineering Research Council of Canada, the Canadian Foundation for Innovation, Ontario Innovation Trust, AUTO 21^{TM} (a member of the Network of Centres of Excellence of Canada programme) and the Ford Motor Company of Canada.

References

[1] S.K. Khalil, F.J. Wallace, J.G. Hawley, Further developments of a computational model for HSDI diesel engines with high-pressure common rail fuel injection, in: Proceedings of Thiesel, Valencia, Spain, 2002, pp. 471–485.

[2] W.T. Lyn, Study of burning rate and nature of combustion in a diesel engine, in: Proceedings of Ninth International Symposium on Combustion, The Combustion Institute, 1962, pp. 1069–1082.

[3] B.M. Grimm, R.T. Johnson, Review of simple heat release computations, SAE 900445.

[4] R.B. Krieger, G.L. Borman, The computation of apparent heat release for internal combustion engines, in: Proc. Diesel Gas Power, ASME 66-WA/DGP-4, 1966.

[5] J.A. Gatowski, E.N. Balles, K.M. Chun, F.E. Nelson, J.A. Ekchian, J.B. Heywood, Heat release analysis of engine pressure data, SAE 841359.

[6] M.F.J. Brunt, H. Rai, A.L. Emtage, The calculation of heat release energy from engine cylinder pressure data, SAE 981052.

[7] M.F.J. Brunt, K.C. Platts, Calculation of heat release in direct injection diesel engines, SAE 1999-01-0187.

[8] J.B. Heywood, Internal Combustion Engine Fundamentals, McGraw-Hill, USA, 1988.

[9] P.A. Lakshminarayanan, Y.V. Aghav, A.D. Dani, P.S. Mehta, Accurate prediction of the heat release in a modern direct injection diesel engine, Proceedings of the Institute of Mechanical Engineers 216 (2002) 663–675.

[10] U. Asad, M. Zheng, D.S.-K. Ting, R. Kumar, S. Banerjee, G.T. Reader, J. Tjong, Real-time heat release analysis towards on-fly combustion control for diesel engines, in: Proceedings of the Combustion Institute/Canadian Section, Spring Technical Meeting, Waterloo, Canada, 2006.

[11] M. Zheng, Thermal efficiency analyses of diesel low temperature combustion cycles, SAE 2007-01-4019.

[12] R.D. Reitz, W.L. Hardy, An experimental investigation of partially premixed combustion strategies using multiple injections in a heavy-duty diesel engine, SAE 2006-01-0917.

[13] A. Maiboom, X. Tauzia, J.-F. Hétet, Experimental study of various effects of exhaust gas recirculation (EGR) on combustion and emissions of an automotive direct injection diesel engine, Energy 33 (2008) 22–34.

[14] M. Zheng, G.T. Reader, R. Kumar, C. Mulenga, U. Asad, Y. Tan, M. Wang, Adaptive control to improve low temperature diesel engine combustion, in: 12th Diesel Engine-Efficiency and Emission Reduction Conference, 2006.

[15] M.Y. Kim, C.S. Lee, Effect of a narrow fuel spray angle and a dual injection configuration on the improvement of exhaust emissions in a HCCI diesel engine, Fuel 86 (2007) 2871–2880.

[16] C.A. Chryssakis, D.N. Assanis, Effect of multiple injections on fuel-air mixing and soot formation in diesel combustion using direct flame visualization and CFD techniques, ASME ICES2005-1016.

[17] M. Zheng, C. Mulenga, G.T. Reader, M. Wang, D.S.-K. Ting, J. Tjong, Biodiesel engine performance and emissions in low temperature combustion, Fuel 87 (2008) 714–722.

[18] R. Kumar, M. Zheng, U. Asad, G.T. Reader, Heat release based adaptive control to improve low temperature diesel engine combustion, SAE 2007-01-0771.

[19] M. Zheng, R. Kumar, G.T. Reader, Adaptive fuel injection tests to extend EGR limits on diesel engines, SAE 2006-01-3426.

[20] R. Basshuysen, F. Schafer, Internal Combustion Engine Handbook: Basics, Components, Systems, and Perspectives, SAE International, USA, 2004.

[21] J. Bengtsson, P. Strandh, R. Johansson, P. Tunestål, B. Johansson, Control of homogeneous charge compression ignition (HCCI) engine dynamics, Journal of Adaptive Control and Signal Processing 18 (2004) 167–179.

[22] C. Amann, Cylinder pressure measurement and its use in engine research, SAE 852067.

[23] M. Zheng, Thermodynamic modelling and experimental investigation of a synthetic atmosphere diesel engine system, PhD thesis, University of Calgary, Canada, 1993.

[24] G.M. Rassweiler, L. Withrow, Motion pictures of engine flames correlated with pressure cards, SAE Journal (Trans.) 42 (May 1938) 185–204 (Reprinted SAE 800131, 1980).

[25] K. Telborn, A real-time platform for closed-loop control and crank angle based measurement, Masters Thesis, Linköping University, Sweden, 2002.

[26] M. Klein, A Specific Heat Ratio Model and Compression Ratio Estimation, Linköping University, Sweden, 2004.

[27] M.C. Sellnau, F.A. Matekunas, P.A. Battiston, C. Chen-Fang, D.R. Lancaster, Cylinder-pressure-based engine control using pressure-ratio-management and low-cost non-intrusive cylinder pressure sensors, SAE 2000-01-0932.

[28] F. Matekunas, Engine combustion control with ignition timing by pressure management ratio, US Patent No 4622939, November 18, 1986.

[29] D.J. Timoney, Problems with heat release analysis in D.I. Diesel, SAE 870270.

[30] D.J. Timoney, Effects of important variables on measured heat release rates in a D.I. Diesel, SAE 870271.

[31] G.A. Karim, M.O. Khan, An examination of some of the errors normally associated with the calculation of apparent rates of combustion heat release in engines, SAE 710135.

[32] V. Rocco, D.I. Diesel engine in-cylinder pressure data analysis under T.D.C. setting error, SAE 930595.

[33] X. Han, U. Asad, M.C. Mulenga, S. Banerjee, M. Wang, G.T. Reader, M. Zheng, Empirical studies of diesel low temperature combustion on a modern diesel engine, in: Proceedings of the Combustion Institute/Canadian Section, Spring Technical Meeting, Banff, Canada, 2007.